



**Queensland University of Technology**  
Brisbane Australia

This is the author's version of a work that was submitted/accepted for publication in the following source:

Dreischarf, M., Zander, T., Shirazi-Adl, A., Puttlitz, C.M., Adam, C.J., Chen, C.S., Goel, V.K., Kiapour, A., Kim, Y.H., Little, J.P., Park, W.M., Labus, K.M., Wang, Y.H., Wilke, H.J., Rohlmann, A., & Schmidt, H. (2014)

Comparison of eight published static finite element models of the intact lumbar spine : predictive power of models improves when combined together.

*Journal of Biomechanics*, 47(8), pp. 1757-1766.

This file was downloaded from: <http://eprints.qut.edu.au/75896/>

© Copyright 2014 Elsevier Inc.

This is the author's version of a work that was accepted for publication in *Journal of Biomechanics*. Changes resulting from the publishing process, such as peer review, editing, corrections, structural formatting, and other quality control mechanisms may not be reflected in this document. Changes may have been made to this work since it was submitted for publication. A definitive version was subsequently published in *Journal of Biomechanics*, [VOL 47, ISSUE 8, (2014)] DOI: 10.1016/j.biomech.2014.04.002

**Notice:** *Changes introduced as a result of publishing processes such as copy-editing and formatting may not be reflected in this document. For a definitive version of this work, please refer to the published source:*

<http://doi.org/10.1016/j.jbiomech.2014.04.002>

# **Comparison of eight published static finite element models of the intact lumbar spine: Predictive power of models improves when combined together**

M. Dreischarf<sup>1</sup>, T. Zander<sup>1</sup>, A. Shirazi-Adl<sup>2</sup>, C.M. Puttlitz<sup>6</sup>, C.J. Adam<sup>7</sup>, C.S. Chen<sup>3</sup>,  
V.K. Goel<sup>4</sup>, A. Kiapour<sup>4</sup>, Y.H. Kim<sup>5</sup>, K.M. Labus<sup>6</sup>, J.P. Little<sup>7</sup>, W.M. Park<sup>5</sup>,  
Y.H. Wang<sup>3</sup>, H.J. Wilke<sup>8</sup>, A. Rohlmann<sup>1</sup>, H. Schmidt<sup>1,8</sup>

<sup>1</sup> Julius Wolff Institute, Charité – Universitätsmedizin Berlin, Augustenburger Platz 1, 13353 Berlin, Germany

<sup>2</sup> Division of Applied Mechanics, Department of Mechanical Engineering, École Polytechnique, Montréal, Quebec, Canada

<sup>3</sup> Department of Physical Therapy and Assistive Technology, National Yang-Ming University, Taipei, Taiwan

<sup>4</sup> Departments of Bioengineering and Orthopaedic Surgery, Colleges of Engineering and Medicine, University of Toledo, USA

<sup>5</sup> Department of Mathematics, Kyonggi University, Suwon 443-760, Republic of Korea

<sup>6</sup> Orthopaedic Bioengineering Research Laboratory, Colorado State University, USA

<sup>7</sup> Paediatric Spine Research Group, Institute of Health and Biomedical Innovation, Queensland University of Technology, Brisbane, Australia

<sup>8</sup> Institute of Orthopaedic Research and Biomechanics, Ulm, Germany

## **Address of the corresponding author:**

Marcel Dreischarf  
Julius Wolff Institute  
Charité – Universitätsmedizin Berlin  
Augustenburger Platz 1  
13353 Berlin  
Germany

Phone: +49 30 209 34 61 43

Fax: +49 30 2093 46001

E-mail: dreischarf@julius-wolff-institut.de

## Abstract

Finite element (FE) model studies have made important contributions to our understanding of functional biomechanics of the lumbar spine. However, if a model is used to answer clinical and biomechanical questions over a certain population, their inherently large inter-subject variability has to be considered. Current FE model studies, however, generally account only for a single distinct spinal geometry with one set of material properties. This raises questions concerning their predictive power, their range of results and on their agreement with in vitro and in vivo values.

Eight well-established FE models of the lumbar spine (L1-5) of different research centres around the globe were subjected to pure and combined loading modes and compared to in vitro and in vivo measurements for intervertebral rotations, disc pressures and facet joint forces.

Under pure moment loading, the predicted L1-5 rotations of almost all models fell within the reported in vitro ranges, and their median values differed on average by only 2° for flexion-extension, 1° for lateral bending and 5° for axial rotation. Predicted median facet joint forces and disc pressures were also in good agreement with published median in vitro values. However, the ranges of predictions were larger and exceeded those reported in vitro, especially for the facet joint forces. For all combined loading modes, except for flexion, predicted median segmental intervertebral rotations and disc pressures were in good agreement with measured in vivo values. In light of high inter-subject variability, the generalization of results of a single model to a population remains a concern. This study demonstrated that the pooled median of individual model results, similar to a probabilistic approach, can be used as an improved predictive tool in order to estimate the response of the lumbar spine.

*Keywords: validation; finite element model; lumbar spine, verification, sensitivity, inter-subject variability, predictive power*

## 1. Introduction

Accurate and clinically relevant modelling of complex biological systems such as the human lumbar spine remains challenging, yet promising, with the potential to substantially enhance the quality of patient care. Due to its ability to represent intricate systems with material nonlinearities, irregular loading, and geometrical and material domains, the finite element (FE) method has been recognized as an important computational tool in various biomedical fields (Zhang and Teo, 2008) and has been widely adopted for describing spinal biomechanics (Schmidt et al., 2013). In comparison to *in vitro* or *in vivo* approaches, computational methods are advantageous in offering cost efficient and powerful response solutions while at the same time effectively dealing with the ethical concerns related to the use of live animals in experiments. Moreover, use of computational models may greatly diminish the need for experimental investigations that utilize post mortem human and animal specimens. For example, finite element models provide improved insight into the functional mechanisms of the spine by assessing the isolated effect of various parameters independently – a feature that has been invaluable with respect to the design/optimization of spinal implants (Fagan et al., 2002a; Schmidt et al., 2013; Zhang and Teo, 2008).

Despite the proven success of computational studies in other disciplines, the FE method's role in clinical spine research has sometimes been questioned (Viceconti et al., 2005). The uncertainty and high variability of tissue material properties, the anatomical complexity of spinal structures (Panjabi et al., 1992, 1993), and the unknown loading (Rohlmann et al., 2009; Wilke et al., 1998) and boundary conditions, particularly *in vivo*, has cast doubt on the accuracy and reliability of FE model predictions. The inherent geometric and material property differences among individuals and alterations in these parameters due to age, sex and degeneration may limit the widespread applicability of the reported results. To gain confidence in and to enhance the predictive quality of FE models, recommendations have been made on how to develop suitable models in order to address research questions within an adequate degree of predictive accuracy (Anderson et al., 2007; Jones and Wilcox, 2008; Oreskes et al., 1994; Roache, 1998; Viceconti, 2011; Viceconti et al., 2005). These standards comprise three main steps: code verification, sensitivity analyses of uncertain model input parameters, and task-specific validations of the

model. The verification of the code poses the least concern as the vast majority of computational studies nowadays employ extensively verified, commercially available FE software. The analysis of the sensitivity to alterations in geometrical (Dupont et al., 2002; Meijer et al., 2011; Natarajan and Andersson, 1999; Niemeyer et al., 2012; Noailly et al., 2007; Robin et al., 1994), material (Fagan et al., 2002b; Lee and Teo, 2005; Rao and Dumas, 1991; Shirazi-Adl, 1994a; Zander et al., 2004) or loading parameters (Dreischarf et al., 2011; 2012; Rohlmann et al., 2009); however, demands more time and effort and has hence only occasionally been carried out. It has been shown that the range of motion (RoM) of a lumbar motion segment is strongly affected by the disc height (Meijer et al., 2011; Natarajan and Andersson, 1999; Niemeyer et al., 2012; Robin et al., 1994) and material properties (e.g. ligament properties (Zander et al., 2004). Furthermore, appropriate loading conditions (Dreischarf et al., 2011, 2012) are necessary to realistically simulate relevant tasks under maximal voluntary motion measured in vivo (Pearcy, 1985; Pearcy et al., 1984; Pearcy and Tibrewal, 1984; Wilke et al., 2001).

The term ‘validation’ merits attention as it remains controversial. Validation is commonly used to indicate that model predictions are consistent with observations. However, it is intractable to completely validate numerical models because it is not possible to account for the multiplicity of their inherent degrees of freedom in an experiment (Oreskes et al., 1994). It is, however, generally accepted that greater number and diversity of corroborating observations between a model and experimental data increases the probability that the model predictions are not flawed (Oreskes et al., 1994; Viceconti et al., 2005). To increase the confidence in a model, the number of free independent parameters employed to construct the model should remain low to decrease the risk of non-uniqueness. Detailed experimental data on the lumbar spine that would allow for a thorough validation of model predictions remain, however, limited. For example, measurements are often only performed at a single level. Model validation is therefore often performed by comparing the calculated results with the limited data that is available from in vitro studies (Moramarco et al., 2010; Zander et al., 2009). However, experimental setups, specimens, loading and boundary conditions substantially differ among various studies (Brinckmann and Grootenboer, 1991; Kettler et al., 2011; Rohlmann et al., 2001b; Wilke et al., 1994), and these differences are often neglected

with regard to the resulting data. Furthermore, the validation of numerical models should preferably include as many relevant outputs as possible (Woldtvedt et al., 2011), as some may be more sensitive to model assumptions than others under specific loading conditions. Moreover, for clinically relevant parameters such as the facet joint forces (FJF), which have considerable dependence on loading and geometry, almost no in vivo data exist (Wilson et al., 2006). Well established FE models should incorporate the aforementioned three steps to meet the conditions for a meaningful numerical study. Despite these requirements, most FE studies account for only one spinal geometry with one set of material properties and are validated with very few available experimental data. This raises questions with regard to the liability/comparability of their predictions under various conditions, on the range of results of these numerical predictions, and on their agreement with in vitro values. Concerns also exist when attempting to validate predictions with in vivo data under complex combined loading modes (e.g. compression and bending). To address these issues, one may compare the salient predictions of peer-reviewed models obtained under nearly identical loading and boundary conditions. For this purpose and due to the importance and complexity of the lumbar spine, this novel multicentre study was undertaken to compare the results of eight well-established FE models of the lumbar spine that have been developed, validated and applied for many years in different research centres around the globe. Tasks simulated consist of pure and combined bending, torsion and compression loads in order to better compare model predictions with each other and with the published in vitro and in vivo data. The objective is to evaluate the predictive power of individual estimations versus the median of all estimations. It is hypothesized that the median predictions of FE models when combined could more closely approximate the experimental data than the predictions of individual models.

## **2. Materials and Methods**

### **2.1 Inclusion criteria**

Ten different research groups, working in the field of spinal FE modeling were invited to participate in the present study. Only validated models of the lumbar spine (L1-5) that were previously published in peer

reviewed journals were considered. A model was considered to be validated when its predictions compared favorably with available measurements under simple loading conditions. From ten groups, eight agreed to participate, one declined due to lack of resources and one did not respond to the invitation. In the current study, complex combined loading modes were employed, for which not all models were validated previously. Thus, all results of the present study were anonymized to increase the number of participating groups. Only the first author (M.D.) had access to the non-anonymized data, and all research groups agreed to the current publication. The models were arbitrarily numbered from 1 to 8.

## 2.2 Study design

The first part of this study served as an *in vitro* validation attempt. Here, FE models were subjected to pure moments and pure compression under standardized loads recommended in experimental studies (Wilke et al., 1998). Results were compared with previously published *in vitro* values (Brinckmann and Grootenboer, 1991; Rohlmann et al., 2001b; Wilson et al., 2006). The second part served as a validation for the simulation of physiological movements of maximal voluntary motions in different planes. Therefore, previously published loading recommendations were employed, and the results were compared with available *in vivo* data (Pearcy, 1985; Pearcy et al., 1984; Pearcy and Tibrewal, 1984; Wilke et al., 2001) in which subjects were requested to perform maximal motions.

## 2.3 Finite element models of the intact lumbar spine

All osseoligamentous FE models employed in this study included at least five lumbar vertebrae and four intervertebral discs (L1-5, Fig. 1). FE models simulated the intact lumbar spine under static loading conditions. Detailed information about the geometry, material properties and validation of each model are described elsewhere (Ayturk and Puttlitz, 2001; Kiapour et al., 2012a; Little et al., 2008, Liu et al., 2011; Park et al., 2013; Schmidt et al., 2012; Shirazi-Adl, 1994b; Zander et al., 2009). For a better evaluation of all models, Tables 1 and 2 list the global mechanical and geometrical properties of the employed FE models.

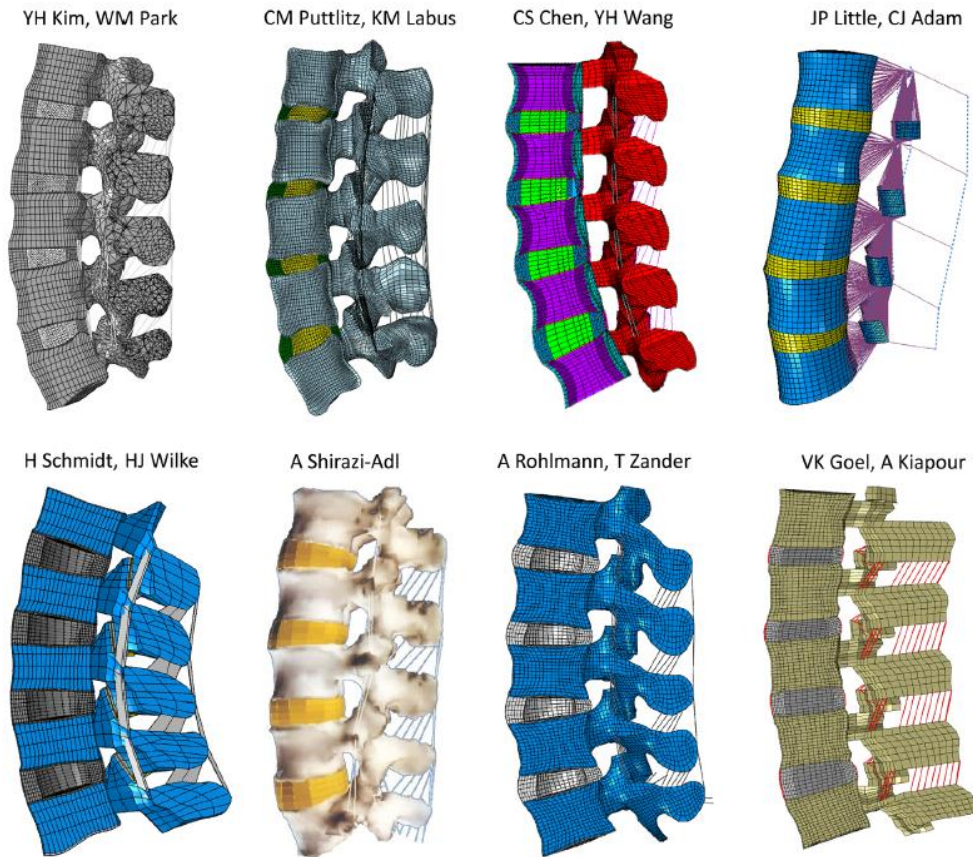


Fig. 1. Finite element models of the L1-5 lumbar spine of all eight participating groups.

**Table 1**  
Mechanical properties of different finite element models.

Component	Kim and Park	Puttitz and Labus	Chen and Wang	Little and Adam	Schmidt and Wilke	Shirazi-Adl	Rohlmann and Zander	Goel and Kiapour
Cortical bone	$E = 12,000 \text{ MPa}$ $\nu = 0.3$	$E_{11} = 8000 \text{ MPa}$ $E_{22} = 8000 \text{ MPa}$ $E_{33} = 12,000 \text{ MPa}$ $\nu_1 = 0.4$ $\nu_2 = 0.35$ $\nu_3 = 0.3$	$E_1 = 22,000 \text{ MPa}$ $E_2 = 11,300 \text{ MPa}$ $\nu_1 = 0.484$ $\nu_2 = 0.203$	$E = 11,300 \text{ MPa}$ $\nu = 0.2$	$E_1 = 22,000 \text{ MPa}$ $E_2 = 11,300 \text{ MPa}$ $\nu_1 = 0.484$ $\nu_2 = 0.203$	Rigid	$E = 10,000 \text{ MPa}$ $\nu = 0.3$	$E = 12,000 \text{ MPa}$ $\nu = 0.3$
Cancellous bone	$E = 100 \text{ MPa}$ $\nu = 0.2$	Based on CT images	$E_1 = 200 \text{ MPa}$ $E_2 = 140 \text{ MPa}$ $\nu_1 = 0.45$ $\nu_2 = 0.315$	$E = 140 \text{ MPa}$ $\nu = 0.2$	$E_1 = 200 \text{ MPa}$ $E_2 = 140 \text{ MPa}$ $\nu_1 = 0.45$ $\nu_2 = 0.315$	Rigid	$E_1 = 200 \text{ MPa}$ $E_2 = 140 \text{ MPa}$ $\nu_1 = 0.45$ $\nu_2 = 0.315$	$E = 100 \text{ MPa}$ $\nu = 0.2$
Posterior bony elements	$E = 3500 \text{ MPa}$ $\nu = 0.25$	$E = 3500 \text{ MPa}$ $\nu = 0.3$	$E = 3500 \text{ MPa}$ $\nu = 0.25$	Quasi-rigid	$E = 3500 \text{ MPa}$ $\nu = 0.25$	Rigid, attached to vertebral body by two deformable beams	$E = 3500 \text{ MPa}$ $\nu = 0.25$	$E = 3500 \text{ MPa}$ $\nu = 0.25$
Ground substance of annulus bulk	Hyperelastic Mooney-Rivlin $c_1 = 0.18$ $c_2 = 0.045$	Hyperelastic/Voeh $c_{10} = 0.0146$ $c_{20} = -0.0189$ $c_{30} = 0.041$	Hyperelastic Mooney-Rivlin $c_1 = 0.42$ $c_2 = 0.105$	Hyperelastic Mooney-Rivlin $c_1 = 0.7$ $c_2 = 0.2$	Hyperelastic Mooney-Rivlin $c_1 = 0.56$ $c_2 = 0.14$	Linear hypoelastic $E = 4.2 \text{ MPa}$ $\nu = 0.45$	Hyperelastic Neo-Hookean $c_1 = 0.3448$ $c_2 = 0.3$	Hyperelastic Neo-Hookean $c_1 = 0.3448$ $c_2 = 0.3$
Nucleus pulposus	Incompressible fluid-filled cavity	$E = 10 \text{ MPa}$ $\nu = 0.49$	Incompressible fluid	Incompressible fluid	Incompressible fluid-filled cavity	Incompressible fluid	Incompressible fluid-filled cavity	Incompressible fluid
Fibers of annulus	Non-linear, dependant on distance from disc center, 6 layers - criss-cross pattern,	Non-linear, two families of fibers $A_3 = 0.03 \text{ (MPa)}$ $b_3 = 120.0 \text{ (unitless)}$	Non-linear, 12 layers - criss-cross pattern,	Tension-only, embedded linear elastic elements, 8 layers with alternating orientation	Non-linear stress-strain curve, 16 layers - criss-cross pattern	8 layers of fiber-reinforced membranes with through annulus depth-dependent thickness and nonlinear properties	Non-linear, dependant on distance from disc center, 14 layers - criss-cross pattern	8 layers of fiber-reinforced continuum elements with criss-cross pattern
Ligaments	Non-linear stress-strain curve	Exponential force-displacement curves	Linear stress-strain curve	Piecewise nonlinear elastic with individual ligament lengths at each spinal level	Non-linear stress-strain curve	Collection of uniaxial elements with nonlinear properties	Non-linear stress-strain curve	Uniaxial 2D elements with theoretically defined cross-sectional area with nonlinear hypoelastic properties
Cartilage of facet joints	Hard frictionless contact, Young's Modulus: 11 MPa, Poisson's ratio: 0.4, Initial gap: 0.5 mm	neo-Hookean, $c_{10} = 2$	Soft contact, Friction coef: 0.1, Initial gap: 0.5 mm	Finite-sliding, frictionless tangential contact with 'softened', exponential normal contact, Initial gap: 0.8 mm	Hard frictionless contact, Young's Modulus: 35 MPa, Poisson's ratio: 0.4, Initial gap: 0.4 mm	Soft frictionless contact with variable gap distances and a gap limit for contact initiation of 1.25 mm	Soft frictionless contact, Initial gap: 0.5 mm	Soft frictionless contact using gap elements with initial clearance of 0.5 mm
Employed data for validation	Panjabi et al. (1994) Guan et al. (2007)	Panjabi et al. (1994) Niosi et al. (2008)  Sawa and Crawford (2008) Ayturk (2007)	Atlas and Deyo (2001) Lin et al. (2013)  McMillan et al. (1996) Yamamoto et al. (1989) Shirazi-Adl (1994c) Chen et al. (2001)	Pearcy (1985) Nachemson (1960)	Heuer et al. (2007b) Heuer et al. (2007a) Rohlmann et al. (2001b) Heuer et al. (2008)	Shirazi-Adl (1994b) Shirazi-Adl (1994c)	Heuer et al. (2007b) Brinckmann and Grootenboer (1991) Rohlmann et al. (2001b) Wilson et al. (2006) Rohlmann et al. (2001a) Wilke et al. (2003)	Kiapour and Goel (2009) Goel et al. (2005) Goel et al. (2007) Kiapour et al. (2012b)
Solver	Abaqus 6.10 <sup>a</sup>	Abaqus 6.11 <sup>a</sup>	ANSYS 11.0 <sup>b</sup>	Abaqus 6.9.1 <sup>a</sup>	Abaqus 6.10 <sup>a</sup>	In-house FE solver	Abaqus 6.10 <sup>a</sup>	Abaqus 6.10 <sup>a</sup>

<sup>a</sup> SIMULIA Inc. Providence, Rhode Island, USA.

<sup>b</sup> Swanson Analysis Systems, Inc, Houston, PA, USA.



**Table 2**  
Geometrical properties of different finite element models.

Component	Kim Park	Putitz Labus	Chen Wang	Little Adam	Schmidt Wilke	Shirazi-Adl	Rohmann Zander	Goel Knapour	Median (range)
Origin of the model	CT-scan of living subject (lying), male, age: 26 years	CT-scan, cadaver specimen, female, age: 49 years	CT-scan of living subject (lying), male, age: 19 years	CT-scans, cadaver specimen, female, age: 59 years	CT-scan, cadaver specimen, male, age: 46 years	CT-scans, cadaver specimen, male, age: 65 years	CT-scan, average values were taken from literature	CT-scan, cadaver specimen, male	30.4 (19.1–44.0)
Lumbar lordosis – L1-L5 Cobb angle (deg)	37	35	27	26.1	44	32.7	28	19.1	
Disc diameter L4-5 (mm)									
lateral	50.8	49	58	39	49	50.3	50	49.8	49.9 (39.0–58.0)
sagittal	33.4	32	43.1	28	35	34.4	37	35.2	34.7 (28.0–43.1)
Disc thickness L4-5 (mm)									
anterior	11.4	16.0	19.4	14	15	15.8	11.5	13.7	14.5 (11.4–19.4)
lateral	7.9	11.1	13.7	9.8	13.5	13.4	9.0	13.2	12.2 (7.9–13.7)
posterior	7.8	7.1	11.2	8.5	12	11.2	6.0	9.2	8.9 (6.0–12.0)
Cross-sectional area L4-5 (mm <sup>2</sup> )									
disc	1460	1332	2075.5	N/A	1380	1455	1480	1210	1455 (1210–2076)
nucleus	560	478	894.6		552	653	624	563	563 (478–895)

## 2.4 Loads and boundary conditions

In 6 of 8 simulations, Dirichlet boundary conditions were applied at the most caudal lumbar vertebra L5 to fix all displacement degrees of freedom. Model 3 and 4 however also included the L5-S1 level and were constrained at the S1 level.

For the first part of this study, pure bending moments of 7.5 Nm were applied in all three anatomical planes (Wilke et al., 1998). For model comparison, the entire L1-5 range of motion (RoM) and the facet joint forces (FJF) at all segments were compared. Subsequently, the FE models were loaded under compression (up to 1000 N) and the L4-5 intradiscal pressure (IDP) predictions were compared. Since the osseoligamentous lumbar spine is inherently unstable (Crisco et al., 1992), the follower load technique was employed (Dreischarf et al., 2010; Parwardhan et al., 1999; Shirazi-Adl and Pamianpour, 2000) to apply the compression. This technique minimizes artifact bending moments expected in compression loading (Crompton et al., 2000).

For the second part, all models were subjected to compression in combination with bending and torsion as shown in Table 3. These loads were taken from FE model studies that simulated most realistically maximal voluntary motions as measured *in vivo* (Pearcy, 1985; Pearcy et al., 1984; Pearcy and Tibrewal, 1984; Wilke et al., 2001). The intervertebral rotations (IVR), IDP values, and FJF were analyzed for each model at all segments. In each model, left and right FJF at all levels were averaged for both sides during extension. In torsion and lateral bending, the sides under higher load were chosen for the sake of comparison.

**Table 3**

Loading modes for the simulation of different body positions.

Body position	Compressive force (N)	Moment (Nm)	References
Flexion	1175	7.5	Rohlmann et al. (2009)
Extension	500	7.5	Rohlmann et al. (2009)
Lateral bending	700	7.8	Dreischarf et al. (2012)
Axial rotation	720	5.5	Dreischarf et al. (2011)

### 3. Results

#### 3.1 Participating groups

Seven of eight groups completed all calculations for the first part of this study. Due to resource limitations, one group only presented results under pure moments and not pure compression. Six of the eight groups participated in the second part as two groups did not participate due to resource limitations. One of the six participating groups was not able to deliver results for the load case upper body flexion, due to convergence problems.

#### 3.2 Part 1 – Pure moments and pure compression

Under pure moments, the median total L1-5 rotation of all FE models (Fig. 2a, each 2<sup>nd</sup> column) differ by only approximately 2° in flexion-extension (FE median: 34°, FE range: 24°-41°), 1° in left-right lateral bending (35°, 25°-41°), and 5° in left-right axial rotation (17°, 11°-22°) from *in vitro* median values (Fig. 2a, red columns). All three FE median values are within the *in vitro* range. Two of eight FE models predict rotations slightly outside the *in vitro* range in flexion-extension and in axial rotation. In lateral bending, all eight models are within the measured range. All FE models demonstrate, albeit to different degrees, a stiffening effect with increasing load resulting in non-linear moment-rotation curves (Fig. 2b).

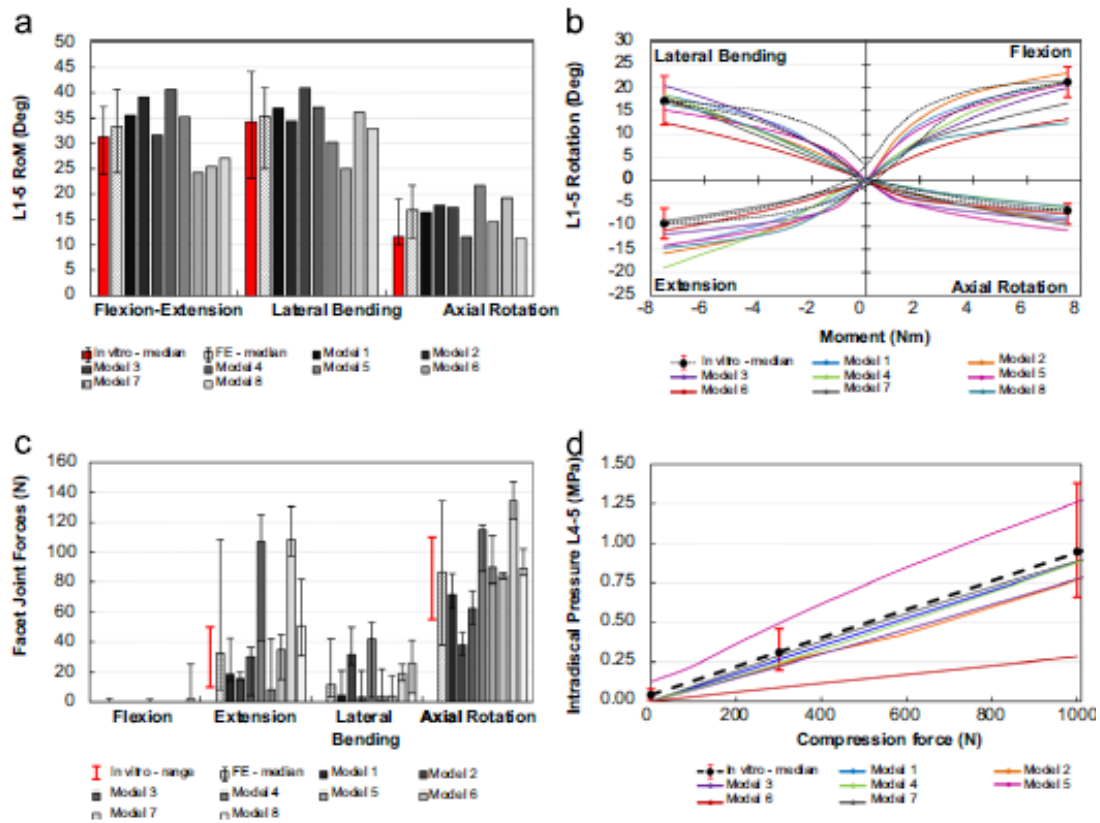


Figure 2. : a) L1-5 range of motion (RoM) under pure moments (3rd to 10th bar). The second dotted bar represents the median value of all eight models and its range represents the range of results of all models. The red bars show the *in vitro* median value and the range of results of ten L1-5 specimens (Rohlmann et al., 2001b). b) Non-linear load-deflection curves (L1-5) of all eight models under pure moments. Black dotted lines represent the median curves of ten L1-5 specimens (Rohlmann et al., 2001b). The red ranges represent their range of results for a moment of 7.5 Nm. c) Median facet joint forces of all spinal levels (L1-5) for each finite element model (2nd to 9th bar), whereas the ranges represent minimal and maximal forces predicted in each model. The dotted bars demonstrate the median facet joint forces of all eight finite element models and their ranges. The red ranges represent the range of facet joint force measured *in vitro* in L1-5 specimens (Wilson et al., 2006). d) Predicted intradiscal pressure in L4-5 nucleus vs. applied compression force. Red black dotted line and red ranges represent the median relationship for five L4-5 segments and its range of results for 0 N, 300 N and 1000 N, respectively (Brinckmann and Grootenboer, 1991).

Median FJF of all levels differ considerably between the models in all moment loading cases (Fig. 2c). Furthermore, the FJF between the levels considerably vary within the models. In extension and axial rotation, two of seven models predict FJF well outside of the *in vitro* range. The segmental FJF of all models are on average 0 N in flexion, 32 N in extension, 12 N in lateral bending and 87 N in axial rotation (Fig. 2c). The medians of the predicted FJF are very close to the centre of the experimentally measured ranges (Fig. 2c, shown in red error bars) for extension (*in vitro*: 30 N, FE-median: 32 N) and axial rotation (*in vitro*: 83 N, FE-median: 87 N). However, the FJF ranges predicted by all models exceed the *in vitro* data range.

Results of all models indicate that under axial compressive loading, the IDP increases almost linearly with the applied load (Fig. 2d). Six of seven models predict L4-5 IDP within the *in vitro* range under 1000 N compression. Only one model considers an initial IDP offset at 0 N (model 5: 0.13 MPa), which leads to IDP values slightly out of range at compression of 300 N. One model predicts IDP values smaller than experimental measured values.

### 3.3 Part 2 – Combined compression-bending and compression-torsion

Except for combined flexion, all predicted segmental median IVRs are within the *in vivo* measured range (Fig. 3 a-d; each red and dotted bar). In flexion, under 7.5 Nm moment and 1175 N compression, all FE models predict smaller IVR than seen *in vivo* under maximal voluntary bending with maximal deviations of approximately 9°. Only for the segment L1-2 are the predictions within the *in vivo* range. The predictions of all FE studies are, however, very similar. For lateral bending and axial rotation, all segmental IVRs of all FE models are within the *in vivo* range and close to the *in vivo* median values. For extension, almost all predicted IVR are within the *in vivo* ranges, except for one case at L1-2 and one at L4-5.

Median FE values of IDP predicted at L4-5 disc are close to the corresponding *in vivo* values for lateral bending, extension and axial rotation (Fig 4, each red and dotted bar). The predicted median IDP for flexion is slightly smaller than what has been measured *in vivo*. There are large variations in the predicted IDP values between all models, especially in extension. It has to be noted that the *in vivo* pressure data were measured in one single subject (Wilke et al., 2001) under maximal voluntary motion.

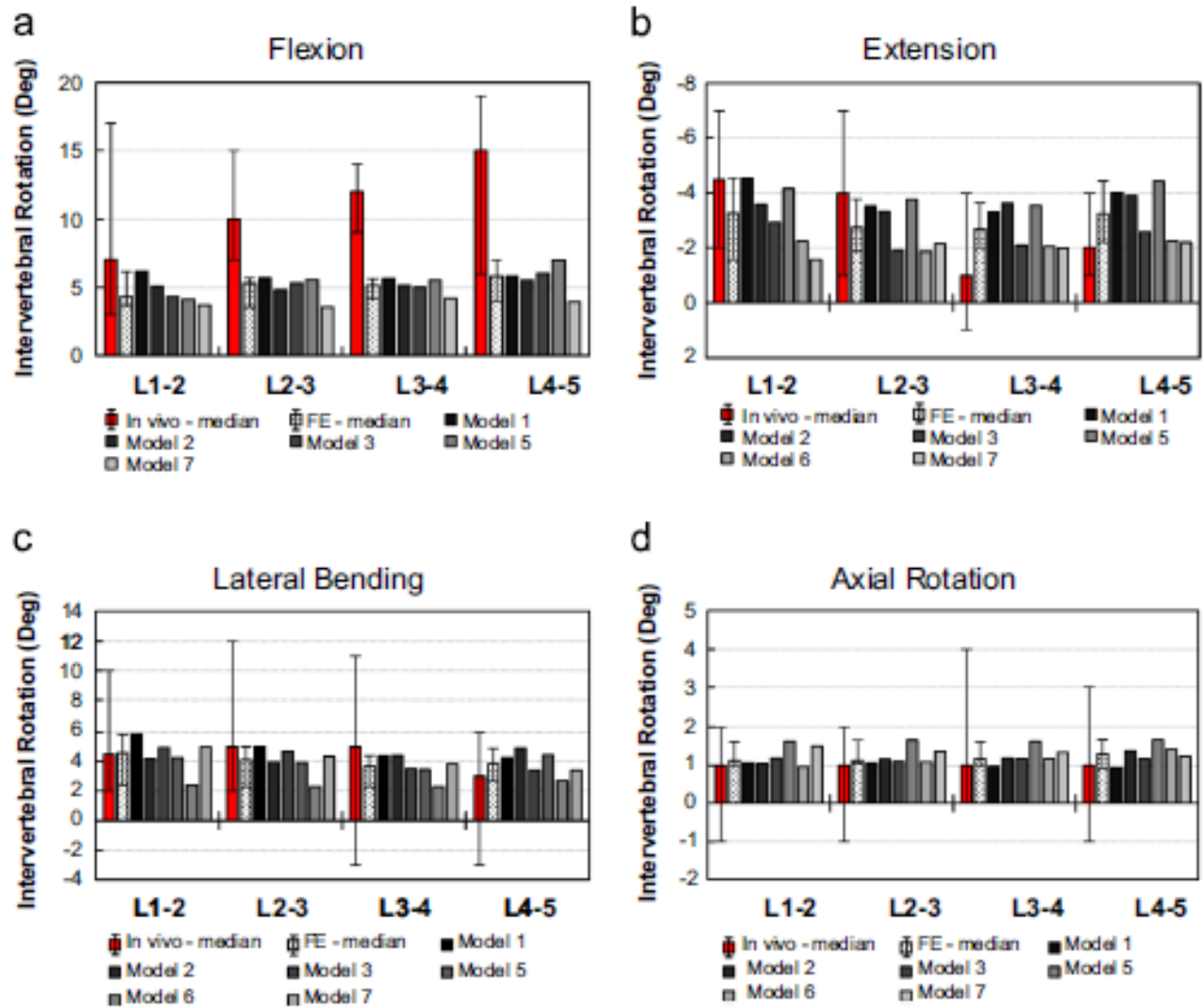


Figure 3. Comparison between predicted intervertebral rotations in different spinal levels of up to six finite element models and median *in vivo* values (Pearcy and Tibrewal, 1984; Percy et al., 1984; Percy, 1985) (red bars) for the loading cases flexion (a), extension (b), lateral bending (c) and axial rotation (d). The dotted bars represent the segmental median values of all models and their range of results.

Predicted total FJF of all FE models are, on average, approximately 38 N in extension, 14 N in lateral bending and 60 N in axial rotation (Fig. 5). In flexion, the facet joints remain unloaded. Computed FJF considerably differ between FE models, especially in lateral bending. Under these combined loading conditions, no measured FJF has been reported, making comparison of these predictions intractable.

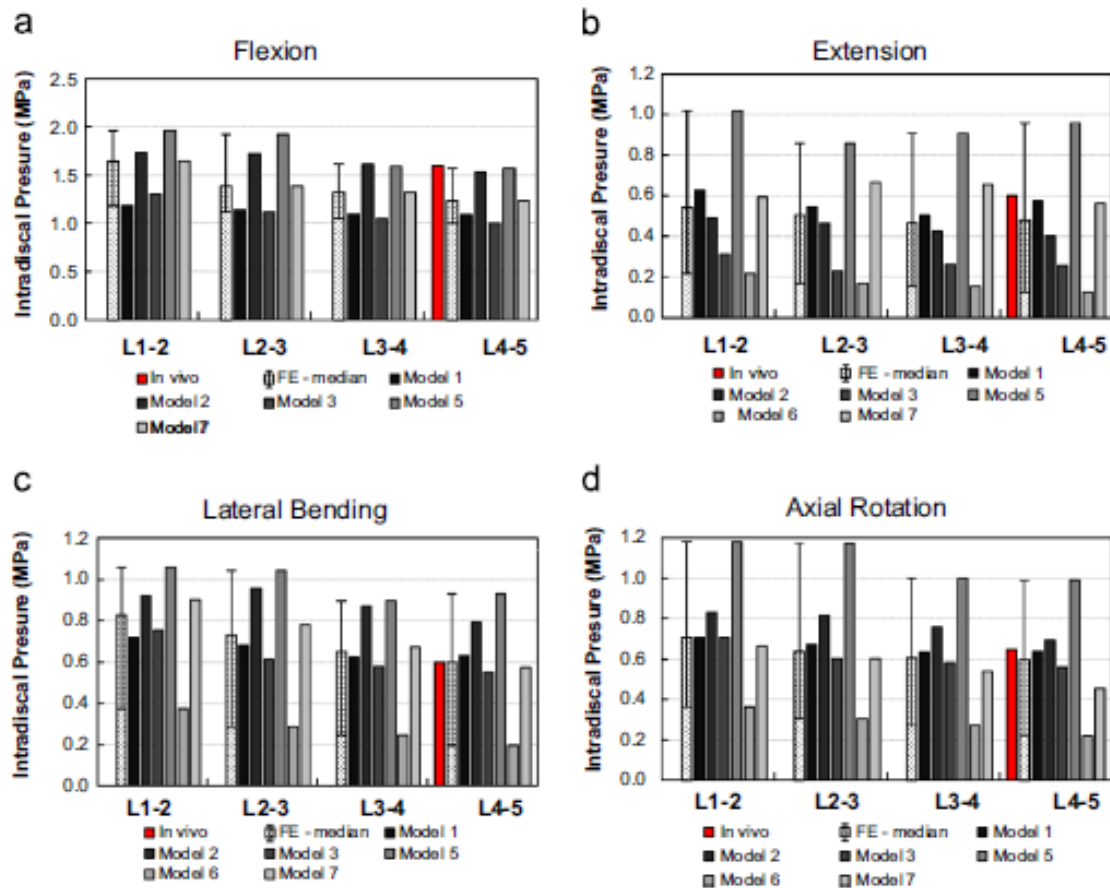
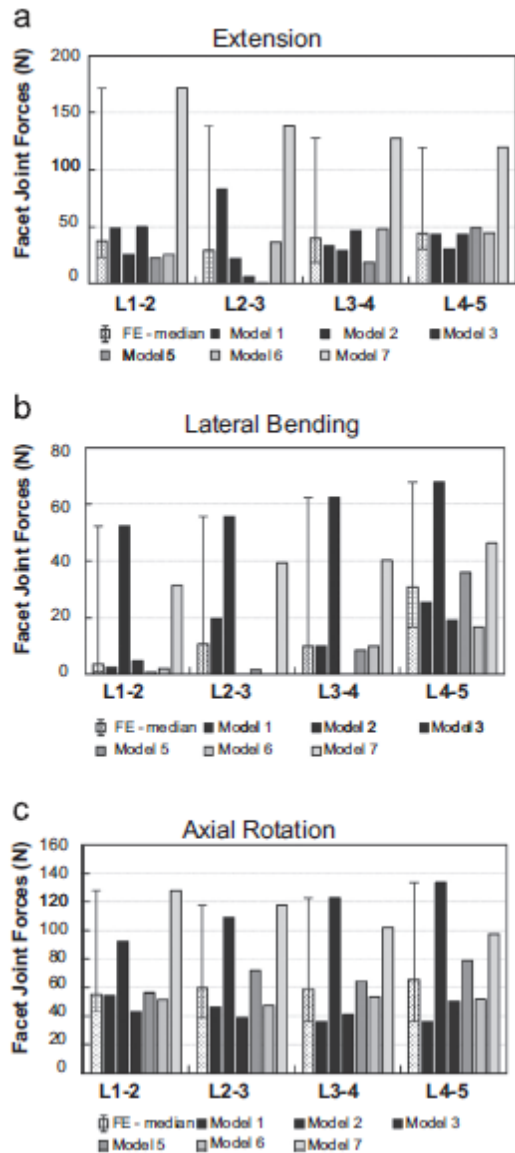


Figure 4. Comparison between predicted intradiscal pressures in different spinal levels for flexion (a), extension (b), lateral bending (c) and axial rotation (d) of up to six finite element models compared to *in vivo* measurements (red bars) by Wilke et al. (2001). The dotted bar represents the segmental median value of all finite element models and their range of results.

#### 4. Discussion

Over the last few decades, the finite element method has been used to investigate the biomechanical behavior of the lumbar spine. These FE models are usually based on only one specific or one idealized average subject with unique mechanical and geometrical characteristics. Thus, with a few exceptions (Little and Adam, 2013; Niemeyer et al., 2012), the effect of inter-subject variability in geometry has mostly not been accounted for in modeling efforts. In addition, the crucial role of individualized material properties has not been incorporated due to the lack of appropriate data, although image analysis and its future developments appear promising for providing *in vivo* material coefficients. In order to reduce these confounding effects, experimental measurements with sufficient sample size attempt to account for such variabilities, though they remain limited due to the availability of specimens, inaccessibility of regions of interest and experimental limitations.



**Fig. 5.** Predicted facet joint forces of six finite element models for the loading cases extension (a), lateral bending (b) and axial rotation (c). The dotted bar represents the segmental median value of all finite element models and their range of results.

Under pure moments, almost all models predicted ranges of motion that moderately differ from each other, and these data compared satisfactorily well with experimental median values. Interestingly, the numerical ranges of eight individual models fit the experimental observations well (Fig. 2a). However, the inter-model deviation in predictions increases for parameters, such as the FJF or IDP, that give insights into the internal loading conditions of the lumbar spine but which are difficult to validate with experimental measurements (Fig. 2c-d). However and interestingly, the median of all model predictions was always relatively close to the *in vitro* median values of the IVR, IDP and FJF indicating the improved capability of FE models when grouped together to predict the experimental results (Fig. 2). This is true to a certain extent also for the second part of this study despite the challenge in simulating maximum voluntary trunk rotations in different planes.

An improved insight into the impact of the material and geometrical diversity on the biomechanical behavior of the lumbar spine is essential for an enhanced understanding of spinal mechanics and patient care. This FE model study aimed to estimate the relative predictive power in using a number of published models when comparing to available limited measurements. Towards this goal, the results of eight FE models of the lumbar spine of different research centers were subjected to almost identical loading and boundary conditions. Under pure moment and compressive loading, the results showed that numerical predictions are in good agreement with *in vitro* measurements of IVR, but differ more from each other and from *in vitro* values for IDP and FJF. In support of our hypothesis, the median response of pooled predictions was in better agreement with reported measurements than the individual predictions. Under combined loads, *in vivo* measured values for IVR and IDP were predicted for extension, lateral bending and axial rotation (Figs. 3 and 4).

This study confirms that the employed combined loading modes of extension, lateral bending and axial rotation lead to the median predicted IDP values which are close to *in vivo* measurements (Fig. 4). Furthermore, except for flexion, the employed moments and forces lead to median segmental IVRs which are very close to *in vivo* measurements, especially for axial rotation and lateral bending (Fig. 3). A bending moment of 7.5 Nm is evidently not sufficient to simulate the peak upper body flexion under maximal voluntary motion with segmental IVR of more than 10° as measured *in vivo*. For upper body flexion, a compression force of 1175 N yields IDP values slightly smaller to those measured by Wilke et al. (2001); 1.6 MPa, which was measured under maximal motion. Using the IDP and disc area measured by Wilke et al. (2001), the compressive force under 1.6 MPa in L4-5 can be estimated to approximately 1900 N (Dreisharf et al., 2013). Earlier compression estimations at L5-S1 of about 2200 N (Arjmand et al., 2010) and 2900 N (Bazrgari et al., 2008) may be due to the L5-S1 level rather than L4-5, subject weight and variation in peak flexion. The employed loading modes for extension, lateral bending and axial rotation can be used as a reference for a more physiologically-relevant simulation under maximal voluntary motion. Since there is no *in vivo* measurement of the FJF, the FJF predictions of the FE models cannot be verified.

Despite the aforementioned advantages of numerical models and their value e.g. as a comparative tool for investigating parameter sensitivity and modeling medical implants, these results emphasize the difficulty in confidently drawing biomechanical conclusions from a single FE model for a certain population. On the contrary, *in vitro* models are limited in providing valuable insights into how the lumbar spine functions and fails, but depending on the sample size, account for potential effects of inter-subject variability. If a model aims to predict the behavior of an average subject, it should incorporate average anatomical properties (Table 2; e.g. lumbar lordosis, disc area, disc height) and be validated for biomechanical parameters (e.g. IVR, IDP) to increase predictive confidence. For this, the sensitivity of input parameters with an important influence on the mechanical behavior (Lu et al., 1996; Meijer et al., 2011; Natarajan and Andersson, 1999; Niemeyer et al., 2012; Robin et al., 1994) such as the articular facet orientations (Niemeyer et al., 2012; Woldtvedt et al., 2011) or disc height and area is crucial for validation. Furthermore, the complex combination and interaction of several geometrical and material properties govern the response of a model under a certain load. To assist future research and to help new researchers in the field of spine biomechanics, the employed material properties and average geometrical values from all models are listed in Tables 1 and 2.

For the present study, it has to be noted that two models included also the most distal level L5-S1 and were constrained at the S1 level. This has an effect on the response of the adjacent segment L4-5. Furthermore, the models differ not only in values of certain material properties and laws (e.g. Young's



modulus of cortical bone, ligaments, bony posterior elements), but also in representation of disc nucleus, disc annulus and facet articulations.

In light of high inter-subject variability, one must be cautious when generalizing predictions obtained from one deterministic model. A possible solution to provide robust information of one specific model is to use statistical methods, e.g. factorial and probabilistic designs, to assess the sensitivity and robustness of the model to variations in input parameters and their interactions. However, incorporating all the main geometric parameters of the lumbar spine into a statistical approach would require a fully parameterized model. The development of such a model, however, has proven to be notoriously difficult. One valid option might be to investigate a few subjects that are representative of the population's variability of interest. This gives an indication of the level of variability one may expect in model predictions. In this study, eight of those representative FE models developed during the last decades were, for the first time, combined and employed to estimate its median and range during pure and combined loading modes. This study confirms that by combining several distinct models, the median of individual numerical results can be used as an improved prediction in order to estimate the response of the lumbar spine. In combination with a sophisticated experimental database, the FE method is thus better able to develop its potential to enhance our understanding of the mechanics of the lumbar spine.

## **5. Conflict of interest**

There are no conflicts of interests.

## **6. Acknowledgments**

This study was partly supported by the Deutsche Forschungsgemeinschaft (DFG PU 510/2-1) and by the Bundesinstitut für Sportwissenschaft (MiSpEx – Network)

## 7. References

- Anderson, A.E., Ellis, B.J., Weiss, J.A., 2007. Verification, validation and sensitivity studies in computational biomechanics. *Comp Methods Biomech Biomed Eng.* 10, 171–184.
- Arjmand, N., Gagnon, D., Plamondon, A., Shirazi-Adl, A., Larivière, C., 2010. A comparative study of two trunk biomechanical models under symmetric and asymmetric loadings. *J Biomech.* 43, 485–491.
- Atlas, S.J., Deyo, R.A., 2001. Evaluating and managing acute low back pain in the primary care setting. *J Gen Intern Med.* 16, 120–131.
- Ayturk, U.M., Puttlitz, C.M., 2011. Parametric convergence sensitivity and validation of a finite element model of the human lumbar spine. *Comput Methods Biomech Biomed Eng.* 14, 695–705.
- Ayturk, U., 2007. Development and Validation of a Three Dimensional High Resolution Nonlinear Finite Element Model of an L3/L4 Functional Spinal Unit. Colorado State University, Fort Collins, CO.
- Bazrgari, B., Shirazi-Adl, A., Trottier, M., Mathieu, P., 2008. Computation of trunk equilibrium and stability in free flexion-extension movements at different velocities. *J Biomech.* 41, 412–421.
- Brinckmann, P., Grootenboer, H., 1991. Change of disc height, radial disc bulge, and intra-discal pressure from discectomy. An in vitro investigation on human lumbar discs. *Spine* 16, 641–646.
- Chen, C.S., Cheng, C.K., Liu, C.L., Lo, W.H., 2001. Stress analysis of the disc adjacent to interbody fusion in lumbar spine. *Med Eng Phys.* 23, 483–491.
- Cripton, P.A., Bruehlmann, S.B., Orr, T.E., Oxland, T.R., Nolte, L.P., 2000. In vitro axial preload application during spine flexibility testing: towards reduced apparatus-related artefacts. *J Biomech.* 33, 1559–68.
- Crisco, J.J., Panjabi, M.M., Yamamoto, I., Oxland, T.R., 1992. Euler stability of the human ligamentous lumbar spine. Part II: Experiment. *Clin Biomech.* 7, 27–32.
- Dreischarf, M., Rohlmann, A., Bergmann, G., Zander, T., 2011. Optimised loads for the simulation of axial rotation in the lumbar spine. *J Biomech.* 44, 2323–27.
- Dreischarf, M., Rohlmann, A., Bergmann, G., Zander, T., 2012. Optimised in vitro applicable loads for the simulation of lateral bending in the lumbar spine. *Med Eng Phys.* 34, 777–80.
- Dreischarf, M., Rohlmann, A., Zhu, R., Schmidt, H., Zander, T., 2013. Is it possible to estimate the compressive force in the lumbar spine from intra-discal pressure measurements? A finite element evaluation. *Med Eng Phys.* 35, 1385–90.
- Dreischarf, M., Zander, T., Bergmann, G., Rohlmann, A., 2010. A non-optimized follower load path may cause considerable intervertebral rotations. *J Biomech.* 43, 2625–2628.
- Dupont, P., Lavaste, F., Skalli, W., 2002. The role of disc, facets and fibres in degenerative process: a sensitivity study. *Studies in Health Technology and Informatics* 88, 356–359.
- Fagan, M.J., Julian, S., Mohsen, A.M., 2002a. Finite element analysis in spine research. *Proceedings of the Institution of Mechanical Engineers, Part H. J Eng Med.* 216, 281–298.
- Fagan, M.J., Julian, S., Siddall, D.J., Mohsen, A.M., 2002b. Patient-specific spine models. Part 1: Finite element analysis of the lumbar intervertebral disc— a material sensitivity study. *Proc Inst Mech Eng, Part H. J Eng Med.* 216, 299–314.

Goel, V.K., Grauer, J.N., Patel, T.C., Biyani, A., Sairyo, K., Vishnubhotla, S., Matyas, A., Cowgill, I., Shaw, M., Long, R., Dick, D., Panjabi, M.M., Serhan, H., 2005. Effects of charité artificial disc on the implanted and adjacent spinal segments mechanics using a hybrid testing protocol. *Spine* 30, 2755–2764.

Goel, V.K., Mehta, A., Jangra, J., Faizan, A., Kiapour, Ali, H.R., Fauth, A.R., 2007. Anatomic Facet Replacement System (AFRS) Restoration of Lumbar Segment Mechanics to Intact: A Finite Element Study and in vitro Cadaver Investigation. *SAS J.* 1, 46–54.

Guan, Y., Yoganandan, N., Moore, J., Pintar, F.A., Zhang, J., Maiman, D.J., Laud, P., 2007. Moment-rotation responses of the human lumbosacral spinal column. *J Biomech.* 40, 1975–1980.

Heuer, F., Schmidt, H., Claes, L., Wilke, H.J., 2007a. Stepwise reduction of functional spinal structures increase vertebral translation and intradiscal pressure. *J Biomech.* 40, 795–803.

Heuer, F., Schmidt, H., Claes, L., Wilke, H.J., 2008. A new laser scanning technique for imaging intervertebral disc displacement and its application to modeling nucleotomy. *Clin Biomech.* 23, 260–269.

Heuer, F., Schmidt, H., Klezl, Z., Claes, L., Wilke, H.J., 2007b. Stepwise reduction of functional spinal structures increase range of motion and change lordosis angle. *J Biomech.* 40, 271–280.

Jones, A.C., Wilcox, R.K., 2008. Finite element analysis of the spine: towards a framework of verification, validation and sensitivity analysis. *Med Eng Phys.* 30, 1287–304

Kettler, A., Rohlmann, F., Ring, C., Mack, C., Wilke, H.J., 2011. Do early stages of lumbar intervertebral disc degeneration really cause instability? Evaluation of an in vitro database. *Eur Spine J.* 20, 578–584.

Kiapour, A., Goel, V.K., 2009. Biomechanics of a novel lumbar total motion segment preservation system: a computational and in vitro study. *Bonezone*, 86–90.

Kiapour, A., Ambati, D., Hoy, R.W., Goel, V.K., 2012a. Effect of graded facetectomy on biomechanics of Dynesys dynamic stabilization system. *Spine* 37, E581–E589.

Kiapour, A., Anderson, D.G., Spenciner, D.B., Ferrara, L., Goel, V.K., 2012b. Kinematic effects of a pedicle-lengthening osteotomy for the treatment of lumbar spinal stenosis. *J Neurosurg Spine* 17, 314–320.

Lee, K.K., Teo, E., Chon, 2005. Material sensitivity study on lumbar motion segment (L2-L3) under sagittal plane loadings using probabilistic method. *J Spinal Disord Tech.* 18, 163–170.

Lin, H-M., Pan, Y-N., Liu, C-L., Huang, L-Y., Huang, C-H., Chen, C-S., 2013. Biomechanical comparison of the K-ROD and Dynesys dynamic spinal fixator systems – a finite element analysis. *Bio-med. Mater Eng.* 23, 495–505.

Little, J.P., Adam, C.J., 2013. Geometric sensitivity of patient-specific finite element models of the spine to variability in user-selected anatomical landmarks. *Comput Methods Biomech Biomed Eng.* ePub ahead of print

Little, J.P., DeVisser, H., Pearcy, M.J., Adam, C.J., 2008. Are coupled rotations in the lumbar spine largely due to the osseo-ligamentous anatomy?—a modeling study. *Comput Methods Biomech Biomed Eng.* 11, 95–103.

Liu, C-L., Zhong, Z-C., Hsu, H-W., Shih, S-L., Wang, S-T., Hung, C., Chen, C-S., 2011. Effect of the cord pretension of the Dynesys dynamic stabilisation system on the biomechanics of the lumbar spine: a finite element analysis. *Eur Spine J.* 20, 1850–1858.

- Lu, Y.M., Hutton, W.C., Gharpuray, V.M., 1996. Do bending, twisting, and diurnal fluid changes in the disc affect the propensity to prolapse? A viscoelastic finite element model. *Spine* 21, 2570–2579.
- McMillan, D.W., McNally, D.S., Garbutt, G., Adams, M.A., 1996. Stress distributions inside intervertebral discs: the validity of experimental “stress profilometry”. *Proc Inst Mech Eng Part H. J Eng Med.* 210, 81–87.
- Meijer, G.J.M., Homminga, J., Veldhuizen, A.G., Verkerke, G.J., 2011. Influence of interpersonal geometrical variation on spinal motion segment stiffness: implications for patient-specific modeling. *Spine* 36, E929–E935.
- Moramarco, V., Pérezdel Palomar, A., Pappalettere, C., Doblaré, M., 2010. An accurate validation of a computational model of a human lumbosacral segment. *J Biomech.* 43, 334–342.
- Nachemson, A., 1960. Lumbar intradiscal pressure. Experimental studies on post- mortem material. *Acta Orthop Scand.* 43 (Suppl.), S1–S104.
- Natarajan, R.N., Andersson, G.B., 1999. The influence of lumbar disc height and cross-sectional area on the mechanical response of the disc to physiologic loading. *Spine* 24, 1873–1881.
- Niemeyer, F., Wilke, H.J., Schmidt, H., 2012. Geometry strongly influences the response of numerical models of the lumbar spine – a probabilistic finite element analysis. *J Biomech.* 45, 1414–1423.
- Niosi, C.A., Wilson, D.C., Zhu, Q., Keynan, O., Wilson, D.R., Oxland, TR., 2008. The effect of dynamic posterior stabilization on facet joint contact forces: an in vitro investigation. *Spine* 33, 19–26.
- Noailly, J., Wilke, H-J., Planell, J.A., Lacroix, D., 2007. How does the geometry affect the internal biomechanics of a lumbar spine bi-segment finite element model? Consequences on the validation process. *J Biomech.* 40, 2414–2425.
- Oreskes, N., Shrader-Frechette, K., Belitz, K., 1994. Verification, validation, and confirmation of numerical models in the Earth sciences. *Science* 263, 641–646.
- Panjabi, M.M., Goel, V., Oxland, T., Takata, K., Duranceau, J., Krag, M., Price, M., 1992. Human lumbar vertebrae. Quantitative three-dimensional anatomy. *Spine* 17, 299–306.
- Panjabi, M.M., Oxland, T.R., Yamamoto, I., Crisco, J.J., 1994. Mechanical behaviour of the human lumbar and lumbosacral spine as shown by three-dimensional load–displacement curves. *J Bone Joint Surg. Am.* Vol. 76, 413–424.
- Panjabi, M.M., Oxland, T.R., Takata, K., Goel, V, Duranceau, J., Krag, M., 1993. Articular facets of the human spine. Quantitative three-dimensional anatomy. *Spine* 18, 1298–1310.
- Park, W.M., Kim, K., Kim, Y.H., 2013. Effects of degenerated intervertebral discs on inter-segmental rotations, intra-discal pressures, and facet joint forces of the whole lumbar spine. *Comput Biol Med.* 43, 1234–1240.
- Patwardhan, A.G., Havey, R.M., Meade, K.P., Lee, B., Dunlap, B., 1999. A follower load increases the load-carrying capacity of the lumbar spine in compression. *Spine* 24, 1003–1009.
- Pearcy, M.J., Portek, I., Shepherd, J., 1984. Three-dimensional x-ray analysis of normal movement in the lumbar spine. *Spine* 9, 294–297.
- Pearcy, M.J., 1985. Stereo-radiography of lumbar spine motion. *Acta Orthop Scand Suppl.* 212, 1–45.

- Pearcy, M.J., Tibrewal, S.B., 1984. Axial rotation and lateral bending in the normal lumbar spine measured by three-dimensional radiography. *Spine* 9, 582–587.
- Rao, A.A., Dumas, G.A., 1991. Influence of material properties on the mechanical behaviour of the L5-S1 intervertebral disc in compression: a nonlinear finite element study. *J Biomed Eng.* 13, 139–151.
- Roache, P., 1998. *Verification and Validation in Computational Science and Engineering*. Hermosa publishers, Albuquerque, N.M..
- Robin, S., Skalli, W., Lavaste, F., 1994. Influence of geometrical factors on the behaviour of lumbar spine segments: a finite element analysis. *Eur Spine J.* 3, 84–90.
- Rohlmann, A., Neller, S., Bergmann, G., Graichen, F., Claes, L., Wilke, H.J., 2001a. Effect of an internal fixator and a bone graft on inter-segmental spinal motion and intra-discal pressure in the adjacent regions. *Eur Spine J.* 10, 301–308.
- Rohlmann, A., Neller, S., Claes, L., Bergmann, G., Wilke, H.J., 2001b. Influence of a follower load on intra-discal pressure and inter-segmental rotation of the lumbar spine. *Spine* 26, E557–E561.
- Rohlmann, A., Zander, T., Rao, M., Bergmann, G., 2009. Realistic loading conditions for upper body bending. *J Biomech.* 42, 884–890.
- Sawa, A.G.U., Crawford, N.R., 2008. The use of surface strain data and a neural networks solution method to determine lumbar facet joint loads during in vitro spine testing. *J Biomech.* 41, 2647–2653.
- Schmidt, H., Galbusera, F., Rohlmann, A., Shirazi-Adl, A., 2013. What have we learned from finite element model studies of lumbar intervertebral discs in the past four decades? *J Biomech.* 46, 2342–2355.
- Schmidt, H., Galbusera, F., Rohlmann, A., Zander, T., Wilke, H.J., 2012. Effect of multilevel lumbar disc arthroplasty on spine kinematics and facet joint loads in flexion and extension: a finite element analysis. *Eur Spine J.* 21(Suppl 5), S663–S674.
- Shirazi-Adl, A., 1994a. Analysis of role of bone compliance on mechanics of a lumbar motion segment. *J Biomech Eng.* 116, 408–412.
- Shirazi-Adl, A., 1994b. Biomechanics of the lumbar spine in sagittal/lateral moments. *Spine* 19, 2407–2414.
- Shirazi-Adl, A., 1994c. Nonlinear stress analysis of the whole lumbar spine in torsion—mechanics of facet articulation. *J Biomech.* 27, 289–299.
- Shirazi-Adl, A., Parnianpour, M., 2000. Load-bearing and stress analysis of the human spine under a novel wrapping compression loading. *Clin Biomech.* 15, 718–725.
- Viceconti, M., 2011. A tentative taxonomy for predictive models in relation to their falsifiability. *Philos Trans Ser A Math Phys Eng Sci.* 369, 4149–4161.
- Viceconti, M., Olsen, S., Nolte, L-P., Burton, K., 2005. *Extr Clin Relev Data Finite Elem Simul.* 20, 451–454.
- Wilke, H., Neef, P., Hinz, B., Seidel, H., Claes, L., 2001. Intra-discal pressure together with anthropometric data – a dataset for the validation of models. *Clin Biomech.* 16 (Suppl 1), S111–S126.
- Wilke, H.J., Claes, L., Schmitt, H., Wolf, S., 1994. A universal spine tester for in vitro experiments with muscle force simulation. *Eur Spine J.* 3, 91–97.

- Wilke, H.J., Wenger, K., Claes, L, 1998. Testing criteria for spinal implants: recommendations for the standardization of in vitro stability testing of spinal implants. *Eur Spine J.* 7, 148–154.
- Wilke, H.J., Rohlmann, A., Neller, S., Graichen, F., Claes, L., Bergmann, G., 2003. ISSLS prize winner: A novel approach to determine trunk muscle forces during flexion and extension: a comparison of data from an in vitro experiment and in vivo measurements. *Spine* 28, 2585–2593.
- Wilson, D.C., Niosi, C.A., Zhu, Q.A., Oxland, T.R., Wilson, D.R., 2006. Accuracy and repeatability of a new method for measuring facet loads in the lumbar spine. *J Biomech* 39, 348–353.
- Woldtvedt, D.J., Womack, W., Gadowski, B.C., Schuldt, D., Puttlitz, C.M., 2011. Finite element lumbar spine facet contact parameter predictions are affected by the cartilage thickness distribution and initial joint gap size. *J Biomech Eng.* 133, 061009.
- Yamamoto, I., Panjabi, M.M., Crisco, T., Oxland, T., 1989. Three-dimensional movements of the whole lumbar spine and lumbosacral joint. *Spine* 14, 1256–1260.
- Zander, T., Rohlmann, A., Bergmann, G., 2004. Influence of ligament stiffness on the mechanical behaviour of a functional spinal unit. *J Biomech.* 37, 1107–1111.
- Zander, T., Rohlmann, A., Bergmann, G., 2009. Influence of different artificial disc kinematics on spine biomechanics. *Clin Biomech.* 24, 135–142.
- Zhang, Q.H., Teo, E., Chon, E., 2008. Finite element application in implant research for treatment of lumbar degenerative disc disease. *Med Eng Phys* 30, 1246–1256.